


Specific heat and thermal conductivity of the triangular-lattice rare-earth material $\text{KBaYb}(\text{BO}_3)_2$ at ultralow temperature

B. L. Pan,¹ J. M. Ni,¹ L. P. He,¹ Y. J. Yu,¹ Y. Xu,^{2,*} and S. Y. Li^{1,3,†}

¹State Key Laboratory of Surface Physics, Department of Physics, Fudan University, Shanghai 200438, China

²Physik-Institut, Universität Zürich, Winterthurerstrasse 190, CH-8057 Zürich, Switzerland

³Collaborative Innovation Center of Advanced Microstructures, Nanjing 210093, China

 (Received 15 October 2020; revised 22 February 2021; accepted 23 February 2021; published 8 March 2021)

We present the ultralow-temperature specific-heat and thermal-conductivity measurements on single crystals of the triangular rare-earth lattice material $\text{KBaYb}(\text{BO}_3)_2$. Our experiments show the absence of long-range magnetic order down to 50 mK, giving the possibility of a quantum spin liquid ground state in this frustrated compound. Furthermore, no signature of spin freezing is observed down to 50 mK in the ac susceptibility measurements. However, no notable contributions from gapless magnetic excitations, but only a Schottky anomaly is observed in the specific-heat data. The ultralow-temperature thermal-conductivity data show that the residual linear term at zero field is negligible, and the thermal conductivity is insensitive to the magnetic field up to 9 T. The ground state of this frustrated triangular rare-earth lattice material is discussed.

DOI: [10.1103/PhysRevB.103.104412](https://doi.org/10.1103/PhysRevB.103.104412)

I. INTRODUCTION

In geometrically frustrated magnetic systems, localized magnetic moments interact through competing exchange interactions that cannot be simultaneously satisfied [1]. Under certain conditions, exotic magnetic ground states have been proposed in this system, such as quantum spin liquids (QSLs). It is a highly entangled quantum state, in which long-range magnetic order is forbidden even down to absolute zero temperature due to strong quantum fluctuations [1–5]. Furthermore, the fractionalized quasiparticles excitations are more fascinating characters of a QSL, and the detection of these excitations is of great importance to identify a QSL material in experiments [1–5].

As the prototype of a QSL in Anderson's resonating valence bond (RVB) model [6], the spin-1/2 triangular lattice Heisenberg antiferromagnet is one of the most promising magnetic systems for searching QSL candidates due to its strong frustration. Experimentally, two organic compounds κ -(BEDT-TTF)₂Cu₂(CN)₃ [7–9] and EtMe₃Sb[Pd(dmit)₂]₂ [10–12] are considered as potential triangular lattice QSL candidates. In particular, after the discovery of YbMgGaO₄ [13], the inorganic Yb-based triangular lattice material has come to the fore as a new platform to study frustrated magnets [13–22]. In YbMgGaO₄, although the huge magnetic specific heat and the excitation continuum observed in inelastic neutron-scattering measurements indicate a possible spinon Fermi surface [13,14], the absence of magnetic thermal conductivity and the spin-glass behavior due to the intrinsic Mg-Ga site disorders cast doubts on such scenarios [15,16]. With the ongoing hot debate about its identity as a

QSL candidate, searching for new triangular rare-earth lattice QSL candidates is of great interest.

Recently, the triangular rare-earth lattice family of $\text{ABaX}(\text{BO}_3)_2$ ($A = \text{Na, K, Rb}$, X is a rare-earth ion) was synthesized and characterized [23–27]. For $X = \text{Yb}$, the absence of long-range magnetic order in $\text{KBaYb}(\text{BO}_3)_2$ [25] and $\text{RbBaYb}(\text{BO}_3)_2$ [26] is confirmed down to 1.8 and 0.37 K, respectively. In particular, in $\text{NaBaYb}(\text{BO}_3)_2$ [27], a second-order phase transition at 0.41 K is observed in specific heat, which can be suppressed in a small field of 0.1 T. The preponderance of the magnetic entropy is unaccounted for at zero field down to the lowest temperature 0.15 K, leaving the possibility of exotic magnetism open. However, the Ba^{2+} and K^+ ions are disordered on the same site in $\text{KBaYb}(\text{BO}_3)_2$ [23], raising the concern whether the spins are frozen like YbMgGaO_4 . In addition, the magnetic excitations in it are still unclear and the lowest temperature 1.8 K cannot satisfy the study of its ground state. Thus, ultralow-temperature specific-heat and thermal-conductivity measurements are desired for figuring out the ground state of $\text{KBaYb}(\text{BO}_3)_2$.

Ultralow-temperature specific-heat and thermal-conductivity measurements have proven to be powerful methods in the study of low-lying excitations in QSL candidates [8,9,11,12]. For example, the specific-heat measurements show low-energy excitations existing in κ -(BEDT-TTF)₂Cu₂(CN)₃, suggesting its gapless feature [8]. The thermal conductivity data, however, reveal the possibility of a tiny gap opening [9].

In this paper, we report the ultralow-temperature specific-heat and thermal-conductivity measurements of high-quality $\text{KBaYb}(\text{BO}_3)_2$ single crystals and we use nonmagnetic isostructural material $\text{KBaLu}(\text{BO}_3)_2$ as a phonon background to study the magnetic specific heat of $\text{KBaYb}(\text{BO}_3)_2$. In specific-heat measurements, the signature of long-range

*yangxu@physik.uzh.ch

†shiyani_li@fudan.edu.cn

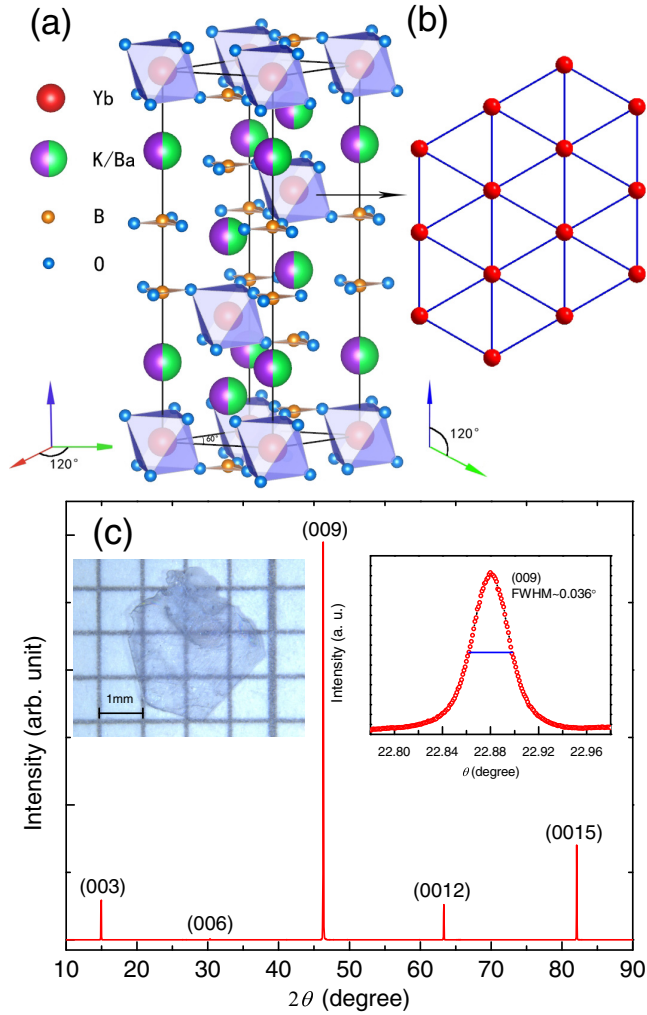


FIG. 1. (a) The unit cell of $\text{KBaYb}(\text{BO}_3)_2$ (K/Ba: purple/green; Yb: red; B: yellow; O: blue). BO_3 units and YbO_6 octahedrons are presented by triangles and purple octahedrons, respectively. (b) Schematic of an extended triangular layer of Yb^{3+} ions viewed along the c axis. (c) Room-temperature x-ray diffraction pattern from the largest natural surface of $\text{KBaYb}(\text{BO}_3)_2$ single crystal. Left inset shows a photograph of a $\text{KBaYb}(\text{BO}_3)_2$ single crystal. Right inset shows the rocking curve of the (009) Bragg peak.

magnetic ordering is found to be absent down to 50 mK and no notable contribution from magnetic excitations is observed besides the Schottky anomaly. Moreover, the κ_0/T at all fields is negligible in thermal conductivity, which shows the absence of itinerant fermionic magnetic excitations in $\text{KBaYb}(\text{BO}_3)_2$ and is consistent with the results of specific heat. Additionally, the thermal conductivity is insensitive to magnetic fields up to 9 T. We shall discuss the possible ground state of $\text{KBaYb}(\text{BO}_3)_2$.

II. EXPERIMENT

Single crystals of $\text{KBaYb}(\text{BO}_3)_2$ were obtained by high-temperature flux growth through spontaneous crystallization [24]. The hexagon single crystal exhibits a mirror-like cleaved surface, as shown in the left inset of Fig. 1(c). The

large natural surface is identified to be the (00 l) plane by a D8 Advance x-ray diffractometer (XRD) from Bruker using the $\text{Cu-K}\alpha$ edge with a wavelength of 1.54 Å, as illustrated in Fig. 1(c). The right inset of Fig. 1(c) shows that the full width at half maximum (FWHM) is only 0.036° , indicating the high quality of the samples. The dc susceptibility measurements were performed in a magnetic property measurement system (MPMS, Quantum Design). The ac susceptibility was measured in the physical property measurement system (PPMS, Quantum Design) equipped with an ac measurement system for the dilution refrigerator option. The applied driving ac magnetic field was 1 Oe. The specific heat was measured by the relaxation method in the physical property measurement system. The single crystals for thermal-conductivity measurements have the dimensions of $3.50 \times 0.81 \times 0.06 \text{ mm}^3$ for sample A, and $2.21 \times 0.43 \times 0.08 \text{ mm}^3$ for sample B, respectively. The two samples used for thermal-conductivity measurements come from two different batches. The thermal conductivity was measured in a dilution refrigerator using a standard four-wire steady-state method with two RuO_2 chip thermometers, calibrated *in situ* against a reference RuO_2 thermometer. Magnetic fields were applied along c axis for both the specific-heat and thermal-conductivity measurements. For comparison, the thermal conductivity of $\text{KBaLu}(\text{BO}_3)_2$ single crystal was also measured on a sample with size of $3.55 \times 0.55 \times 0.13 \text{ mm}^3$.

III. RESULTS AND DISCUSSION

$\text{KBaYb}(\text{BO}_3)_2$ crystallizes in the space group $R\bar{3}m$ [23]. As shown in Fig. 1(a), interlinked between flat BO_3 triangles are double sheets of K or Ba ions and single sheets of YbO_6 octahedrons. The YbO_6 octahedrons and the BO_3 triangles are corner-sharing. As emphasized in Fig. 1(b), the rare-earth ions make up discrete triangular layers within the ab plane. Triangular layers of YbO_6 octahedrons are ABC stacked along the c axis.

The temperature dependence of the dc susceptibility at $\mu_0 H = 0.5$ T applied parallel and perpendicular to the c axis of $\text{KBaYb}(\text{BO}_3)_2$ single crystal are plotted in Fig. 2(a). No anomaly is observed, indicating the absence of magnetic phase transition from 300 to 2 K. The inset of Fig. 2(a) presents the temperature dependence of inverse dc susceptibility at $\mu_0 H = 0.5$ T. The data below 12 K can be fit to the Curie-Weiss law. The Curie-Weiss fit gives the Weiss temperature $\theta_\perp = -0.53$ K and $\theta_\parallel = -0.35$ K, consistent with previous measurements, suggesting weak antiferromagnetic exchange interactions [25]. If the XXZ model can be adopted to estimate the exchange interaction J in $\text{KBaYb}(\text{BO}_3)_2$, $\theta_\perp = -3J_\pm$ for the field perpendicular to c axis and $\theta_\parallel = -3J_{zz}/2$ for the field parallel to the c axis [22], giving $J_\pm = 0.18$ K and $J_{zz} = 0.23$ K, respectively. The magnetization of $\text{KBaYb}(\text{BO}_3)_2$ at 2 K up to $\mu_0 H = 7$ T is shown in Fig. 2(b). At low fields, the magnetization rapidly increases with external field and then gradually saturates. The saturated magnetization is about $1.2\mu_B$ and $2.1\mu_B$ per Yb^{3+} for the applied fields perpendicular and parallel to the c axis of $\text{KBaYb}(\text{BO}_3)_2$, respectively, consistent with a spin-1/2 system. The Landé g factors can be obtained from the saturation magnetic moments $\mu_{\text{sat}} = gS\mu_B$ with $S = 1/2$, giving

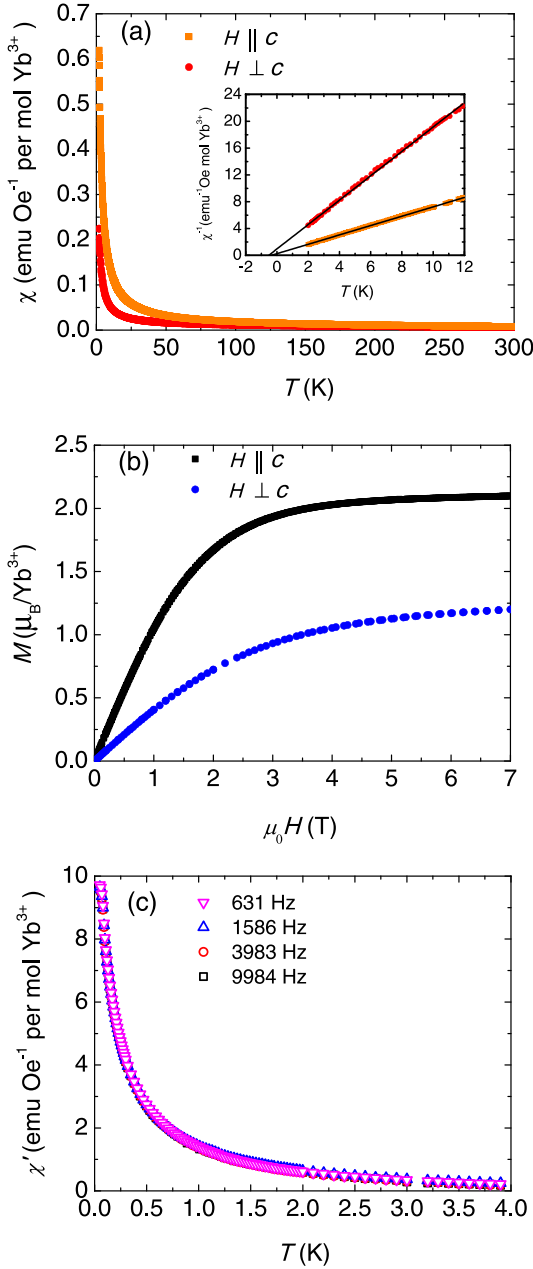


FIG. 2. (a) Temperature dependence of dc susceptibility at $\mu_0 H = 0.5$ T parallel and perpendicular to c axis of $\text{KBaYb}(\text{BO}_3)_2$ single crystal. Inset shows the inverse susceptibility $1/\chi$ at low temperatures. (b) Magnetic-field dependence of the dc magnetization at 2 K with applied fields perpendicular and parallel to c axis of $\text{KBaYb}(\text{BO}_3)_2$. (c) Temperature dependence of real part of ac susceptibility with different driving frequencies. The driving magnetic field is 1 Oe. These data are scaled to dc susceptibility data collected at temperatures above 2 K and fields parallel to c axis. No spin freezing behavior is observed down to 50 mK.

$g_{ab} = 2.4$ and $g_c = 4.2$, respectively. This will be useful in the analysis of the Schottky anomaly in the specific-heat data below. The ac susceptibility measurements from 4 to 0.05 K at different driving frequencies are presented in Fig. 2(c). The Curie-Weiss-like behavior of the real part of ac susceptibility persists down to 50 mK, and no broad peak like YbMgGaO_4

is observed. In addition, the real part of the ac susceptibility is independent of driving frequencies. These results indicate that there is no spin freezing down to the lowest temperatures we measured. Therefore, no spin glass behavior is observed in $\text{KBaYb}(\text{BO}_3)_2$, which is contrary to YbMgGaO_4 . In this context, the disorder between K (or Ba) site may not play an important role in the spin state of $\text{KBaYb}(\text{BO}_3)_2$.

Figure 3(a) shows the specific heat of $\text{KBaYb}(\text{BO}_3)_2$ single crystal at zero field, which is plotted as C/T vs T^2 to present the magnetic excitations (if they exist) more visually. The specific heat of nonmagnetic $\text{KBaLu}(\text{BO}_3)_2$ single crystal is presented for comparison. The C/T curves of $\text{KBaYb}(\text{BO}_3)_2$ and $\text{KBaLu}(\text{BO}_3)_2$ are almost overlapping above 3 K, demonstrating that the specific heat of $\text{KBaLu}(\text{BO}_3)_2$ can be used as the lattice specific heat for $\text{KBaYb}(\text{BO}_3)_2$. We try to fit C/T of $\text{KBaYb}(\text{BO}_3)_2$ by the formula $C/T = \gamma + \beta T^2$ between 3.2 and 5.9 K and extrapolate the fitting line to zero temperature, giving $\gamma = 0.19 \pm 0.19$ mJ K $^{-2}$ mol $^{-1}$ and $\beta = 0.48 \pm 0.01$ mJ K $^{-4}$ mol $^{-1}$. Under normal circumstances, a finite residual linear term γ in specific heat represents the contributions from fermionic excitations in the zero-temperature limit, which may come from a spinon-Fermi surface or nodes in the q space and is considered as a gapless QSL scenario [28,29]. Considering the fitting error bar ± 0.19 mJ K $^{-2}$ mol $^{-1}$ in the specific heat of $\text{KBaYb}(\text{BO}_3)_2$ and comparing with $\gamma \approx 20$ mJ K $^{-2}$ mol $^{-1}$ in κ -(BEDT-TTF) $_2\text{Cu}_2(\text{CN})_3$ [8] and $\text{EtMe}_3\text{Sb}[\text{Pd}(\text{dmit})_2]_2$ [12], the γ is virtually zero, which indicates the absence of gapless magnetic excitations in $\text{KBaYb}(\text{BO}_3)_2$.

The magnetic specific heat of $\text{KBaYb}(\text{BO}_3)_2$ can be extracted by subtracting the lattice contributions C_{lattice} , i.e., the specific heat of $\text{KBaLu}(\text{BO}_3)_2$, from that of $\text{KBaYb}(\text{BO}_3)_2$. The magnetic specific heat of $\text{KBaYb}(\text{BO}_3)_2$ at various magnetic fields are plotted in Fig. 3(b). The peak shifts to higher temperatures and broadens with increasing applied fields, resembling a Schottky anomaly. Especially, the upturn below 0.3 K at zero field may be contributed by the nuclear Schottky effect from Yb nuclei. In finite fields, the magnetic specific heat of $\text{KBaYb}(\text{BO}_3)_2$ can be precisely fit to a two-level Schottky function,

$$C_{\text{Schottky}} = nR \left(\frac{\Delta}{T} \right)^2 \frac{e^{-\frac{\Delta}{T}}}{(1 + e^{-\frac{\Delta}{T}})^2}, \quad (1)$$

where n is the concentration of Schottky centers, R is the gas constant, and Δ is the Zeeman gap of Yb^{3+} electrons in magnetic fields. Taking Δ and n as fitting parameters, the fits for the data above 0.4 K are presented in Fig. 3(b) and give $n \approx 0.9$ under various magnetic fields, which means almost all magnetic ions Yb^{3+} contribute to the Schottky specific heat. As seen in Fig. 3(c), Δ can be plotted as a function of the form $\Delta = 2\mu_{\text{sat},c}B$. $\mu_{\text{sat},c} = g_c S \mu_B$ is the saturation magnetic moment for the $H \parallel c$ axis. This function comes from the Zeeman energy $U = -\mu_{\text{sat},c}B$. The fit gives $\mu_{\text{sat},c} = 1.74 \mu_B$ and $g_c = 3.48$, which is close to the results from the magnetization measurements in Fig. 2(b). This result confirms that the Schottky effect in specific-heat measurements come from the Yb^{3+} Kramers' doublets with effective 1/2 spins.

To exclude the possible case that magnetic excitations are covered by Schottky anomaly in specific heat, we perform the

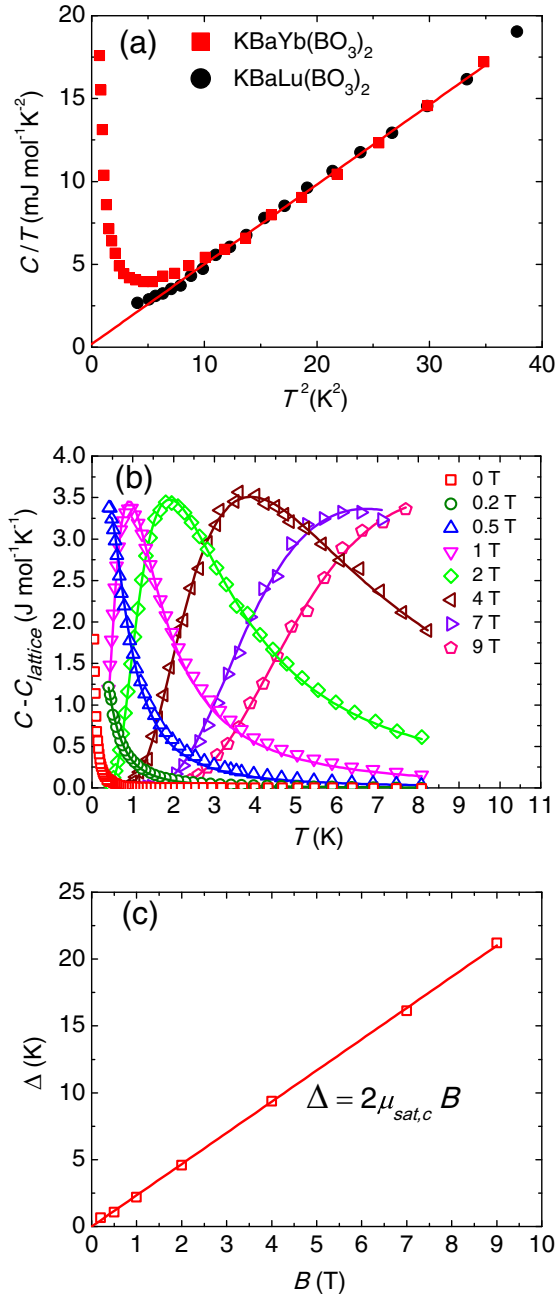


FIG. 3. (a) Zero-field specific heat of $\text{KBaYb}(\text{BO}_3)_2$ and $\text{KBaLu}(\text{BO}_3)_2$ single crystals plotted as C/T vs T^2 . The red line is the fit to the specific-heat data of $\text{KBaYb}(\text{BO}_3)_2$ between 3.2 and 5.9 K to $C/T = \gamma + \beta T^2$. (b) Temperature dependence of magnetic specific heat of $\text{KBaYb}(\text{BO}_3)_2$ at various magnetic fields. Solid lines represent the fits to the two-level Schottky function as described in text after subtracting the lattice contribution C_{lattice} . (c) Magnetic-field dependence of the gap Δ of the two-level system in $\text{KBaYb}(\text{BO}_3)_2$. The red line is the fit to $\Delta = 2\mu_{\text{sat},c} B$.

thermal-conductivity measurements. This method is only sensitive to itinerant excitations and the Schottky anomaly has no effect on it. In a solid, the contributions to thermal conductivity may come from various quasiparticles, such as electrons, phonons, magnons, and spinons. Since $\text{KBaX}(\text{BO}_3)_2$ is an insulator, electrons do not contribute to the thermal conductivity

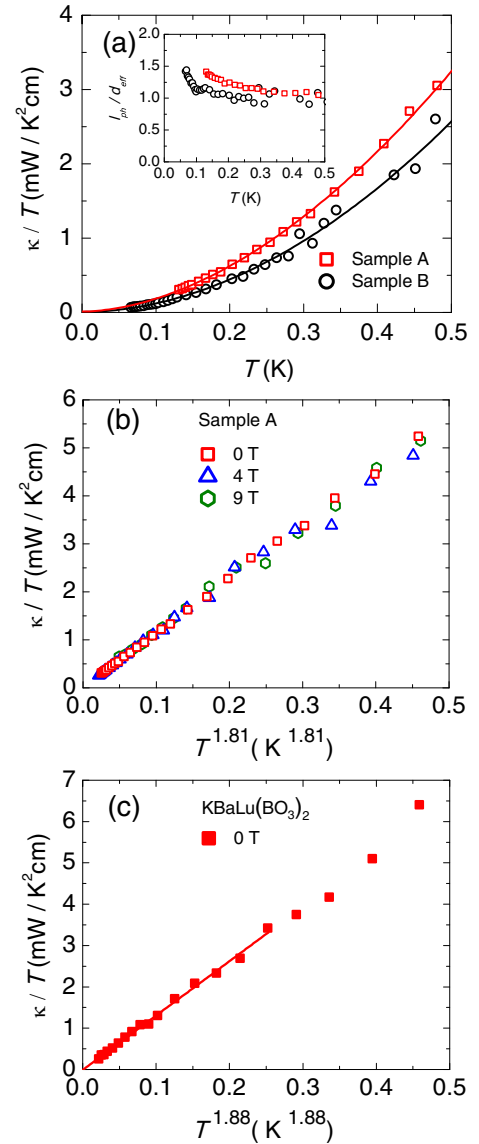


FIG. 4. (a) The in-plane thermal conductivity of two $\text{KBaYb}(\text{BO}_3)_2$ single crystals at $\mu_0 H = 0$ T. The solid line is the fit to the data below 0.5 K to $\kappa/T = a + bT^{\alpha-1}$. Inset shows the temperature dependence of the ratio of phonon mean-free path l_{ph} to effective sample diameter d_{eff} of the two samples. (b) The in-plane thermal conductivity of sample A at various magnetic fields ($\mu_0 H = 0, 4$, and 9 T). (c) The in-plane thermal conductivity of $\text{KBaLu}(\text{BO}_3)_2$ single crystal at $\mu_0 H = 0$ T. The solid line is the fit to the data below 0.5 K to $\kappa/T = a + bT^{\alpha-1}$.

at such low temperatures at all. One also does not need to consider the magnon contributions due to the absence of magnetic order down to 50 mK. Therefore, the ultralow-temperature thermal conductivity of $\text{KBaX}(\text{BO}_3)_2$ can be fit to $\kappa/T = a + bT^{\alpha-1}$, in which the two terms aT and bT^{α} represent the contributions from fermionic magnetic excitations (if they exist) and phonons, respectively [30,31].

Figure 4(a) shows the in-plane thermal conductivity of two $\text{KBaYb}(\text{BO}_3)_2$ single crystals at zero field. As for the phonon scattering, the phonon mean-free path l_{ph} can be estimated by the kinetic formula $\kappa = \frac{1}{3} C_{ph} v_{ph} l_{ph}$, where $C_{ph} = \beta T^3$ is

the phonon specific heat and v_{ph} is the velocity of phonons. With $\beta = 0.48 \text{ mJ mol}^{-1} \text{ K}^{-4}$, taken from the specific-heat measurements, v_{ph} is estimated to be $2.84 \times 10^3 \text{ m/s}$. Therefore, l_{ph} can be estimated. When the sample enters the boundary scattering limit, the effective sample diameter $d_{\text{eff}} = 2\sqrt{A/\pi}$, where A is the cross-sectional area of the sample. These are about $249 \text{ }\mu\text{m}$ and $207 \text{ }\mu\text{m}$ for samples A and B, respectively. The plot of l_{ph}/d_{eff} of samples A and B at zero magnetic field is presented in the inset of Fig. 4(a). As can be seen from the figure, l_{ph} is slightly larger than d_{eff} , indicating that the boundary scattering limit is achieved in both samples. The in-plane thermal conductivity of sample A in magnetic fields applied along the c axis are plotted in Fig. 4(b). The three curves almost overlap with each other, which indicates that the magnetic fields barely have any effect on thermal conductivity up to 9 T. For sample A, we fit the zero-field data below 0.5 K to $\kappa/T = a + bT^{\alpha-1}$, which gives the residual linear term $\kappa_0/T = 0.008 \pm 0.011 \text{ mW K}^{-2} \text{ cm}^{-1}$, and $\alpha = 2.81$. Because of the specular reflections of phonons at the sample surfaces, the power α is typically between two and three [30,31]. Considering our experimental error bar $\pm 5 \text{ }\mu\text{W K}^{-2} \text{ cm}^{-1}$, the residual linear term κ_0/T of sample A is virtually zero in various magnetic fields, indicating the absence of itinerant gapless magnetic excitations. For comparison, as shown in Fig. 4(c), the fitting of in-plane thermal conductivity of $\text{KBaLu}(\text{BO}_3)_2$ at zero field below 0.5 K gives the residual linear term $\kappa_0/T = -0.008 \pm 0.027 \text{ mW K}^{-2} \text{ cm}^{-1}$, and $\alpha = 2.88$. The magnetic field also does not affect the thermal conductivity of this nonmagnetic counterpart up to 9 T (data not shown). To exclude the possibility of sample dependence, the thermal conductivity of another sample B is also plotted in Fig. 4(a). The fitting gives $a = 0.007 \pm 0.016 \text{ mW K}^{-2} \text{ cm}^{-1}$ and $\alpha = 2.93$. The residual linear term κ_0/T is also negligible.

The absence of magnetic specific heat (besides the Schottky anomaly) and magnetic thermal conductivity indicate that there are no gapless magnetic excitations in $\text{KBaYb}(\text{BO}_3)_2$, which are hallmarks to identify a QSL material. Since $\text{KBaYb}(\text{BO}_3)_2$ has a low $J_{\pm} = 0.18 \text{ K}$ and $J_{zz} = 0.23 \text{ K}$, as estimated above, we should observe thermally excited magnetic quasiparticles in case it is a gapped QSL. For other triangular-lattice QSL candidates, J is 250 K in κ -(BEDT-TTF) $_2\text{Cu}_2(\text{CN})_3$ [8], 220–250 K in $\text{EtMe}_3\text{Sb}[\text{Pd}(\text{dmit})_2]_2$ [12], and $J_{\pm} = 4.7 \text{ K}$, $J_{zz} = 2.3 \text{ K}$ in

NaYbSe_2 with the same Yb^{3+} lattice as $\text{KBaYb}(\text{BO}_3)_2$ [32]. These values of J are much higher than that in $\text{KBaYb}(\text{BO}_3)_2$, and these three compounds all show anomalous magnetic specific heat [8,12,33]. In this sense, it is more promising to find QSL candidates with large J among frustrated materials.

Combining the absence of spin freezing from the ac susceptibility measurements down to 50 mK and the absence of mobile gapless excitations from the specific heat and thermal conductivity measurements, spin glass and spin liquid ground states are unlikely in $\text{KBaYb}(\text{BO}_3)_2$. We propose that a cooperative paramagnet without long-range entanglement may be the true ground state of $\text{KBaYb}(\text{BO}_3)_2$. This is quite contrary to another Yb-based triangular lattice material YbMgGaO_4 , where a spin-glass ground state is proposed [16]. This discrepancy may come from the different magnitude of magnetic exchange interactions, which will help to better understand the QSL physics in Yb-based frustrated magnets.

IV. SUMMARY

In summary, we have grown high-quality single crystals of the triangular rare-earth lattice material $\text{KBaYb}(\text{BO}_3)_2$ and measured the ultralow-temperature specific heat and thermal conductivity. Long-range magnetic order is not found down to 50 mK. The ac susceptibility measurements do not show any signatures of spin freezing. The specific heat has a huge field-dependent Schottky anomaly and no other magnetic contributions are observed. The thermal conductivity is insensitive to magnetic fields up to 9 T, and no residual linear term is observed at the zero-temperature limit. These results demonstrate the absence of gapless magnetic excitations and suggest that $\text{KBaYb}(\text{BO}_3)_2$ may not be a good candidate to explore the QSL physics, but a cooperative paramagnet without long-range entanglement, likely due to its low magnetic exchange interactions.

ACKNOWLEDGMENTS

This work was supported by the Natural Science Foundation of China (Grant No. 12034004) and the Ministry of Science and Technology of China (Grant No. 2016YFA0300503).

B.L.P. and J.M.N. contributed equally to this work.

-
- [1] L. Balents, Spin liquids in frustrated magnets, *Nature (London)* **464**, 199 (2010).
 - [2] L. Savary and L. Balents, Quantum spin liquids: A review, *Rep. Prog. Phys.* **80**, 016502 (2017).
 - [3] Y. Zhou, K. Kanoda, and T. K. Ng, Quantum spin liquid states, *Rev. Mod. Phys.* **89**, 025003 (2017).
 - [4] H. Takagi, T. Takayama, G. Jackeli, G. Khaliullin, and S. E. Nagler, Concept and realization of Kitaev quantum spin liquids, *Nat. Rev. Phys.* **1**, 264 (2019).
 - [5] C. Broholm, R. J. Cava, S. A. Kivelson, D. G. Nocera, M. R. Norman, and T. Senthil, Quantum spin liquids, *Science* **367**, eaay0668 (2020).
 - [6] P. W. Anderson, Resonating valence bonds: A new kind of insulator?, *Mater. Res. Bull.* **8**, 153 (1973).
 - [7] Y. Shimizu, K. Miyagawa, K. Kanoda, M. Maesato, and G. Saito, Spin-Liquid State in an Organic Mott Insulator with a Triangular Lattice, *Phys. Rev. Lett.* **91**, 107001 (2003).
 - [8] S. Yamashita, Y. Nakazawa, M. Oguni, Y. Oshima, H. Nojiri, Y. Shimizu, K. Miyagawa, and K. Kanoda, Thermodynamic properties of a spin-1/2 spin-liquid state in a κ -type organic salt, *Nat. Phys.* **4**, 459 (2008).
 - [9] M. Yamashita, N. Nakata, Y. Kasahara, T. Sasaki, N. Yoneyama, N. Kobayashi, S. Fujimoto, T. Shibauchi, and Y. Matsuda, Thermal-transport measurements in a quantum spin-liquid state

- of the frustrated triangular magnet κ -(BEDT-TTF)₂Cu₂(CN)₃, *Nat. Phys.* **5**, 44 (2009).
- [10] T. Itou, A. Oyamada, S. Maegawa, M. Tamura, and R. Kato, Quantum spin liquid in the spin-1/2 triangular antiferromagnet EtMe₃Sb[Pd(dmit)₂]₂, *Phys. Rev. B* **77**, 104413 (2008).
- [11] M. Yamashita, N. Nakata, Y. Senshu, M. Nagata, H. M. Yamamoto, R. Kato, T. Shibauchi, and Y. Matsuda, Highly mobile gapless excitations in a two-dimensional candidate quantum spin liquid, *Science* **328**, 1246 (2010).
- [12] S. Yamashita, T. Yamamoto, Y. Nakazawa, M. Tamura, and R. Kato, Gapless spin liquid of an organic triangular compound evidenced by thermodynamic measurements, *Nat. Commun.* **2**, 275 (2011).
- [13] Y. S. Li, H. Liao, Z. Zhang, S. Li, F. Jin, L. Ling, L. Zhang, Y. Zou, L. Pi, Z. Yang, J. Wang, Z. Wu, and Q. Zhang, Gapless quantum spin liquid ground state in the two dimensional spin-1/2 triangular antiferromagnet YbMgGaO₄, *Sci. Rep.* **5**, 16419 (2015).
- [14] Y. Shen, Y.-D. Li, H. Wo, Y. Li, S. Shen, B. Pan, Q. Wang, H. C. Walker, P. Steffens, M. Boehm, Y. Hao, D. L. Quintero-Castro, L. W. Harriger, L. Hao, S. Meng, Q. Zhang, G. Chen, and J. Zhao, Spinon Fermi surface in a triangular lattice quantum spin liquid YbMgGaO₄, *Nature (London)* **540**, 559 (2016).
- [15] Y. Xu, J. Zhang, Y. S. Li, Y. J. Yu, X. C. Hong, Q. M. Zhang, and S. Y. Li, Absence of Magnetic Thermal Conductivity in the Quantum Spin-Liquid Candidate YbMgGaO₄, *Phys. Rev. Lett.* **117**, 267202 (2016).
- [16] Z. Ma, J. Wang, Z. Y. Dong, J. Zhang, S. Li, S. H. Zheng, Y. Yu, W. Wang, L. Che, K. Ran, S. Bao, Z. Cai, P. Cermak, A. Schneidewind, S. Yano, J. S. Gardner, X. Lu, S. L. Yu, J. M. Liu, S. Y. Li, J. X. Li, and J. Wen, Spin-Glass Ground State in a Triangular-Lattice Compound YbZnGaO₄, *Phys. Rev. Lett.* **120**, 087201 (2018).
- [17] J. A. M. Paddison, M. Daum, Z. L. Dun, G. Ehlers, Y. H. Liu, M. B. Stone, H. D. Zhou, and M. Mourigal, Continuous excitations of the triangular-lattice quantum spin liquid YbMgGaO₄, *Nat. Phys.* **13**, 117 (2017).
- [18] Z. Zhu, P. A. Maksimov, S. R. White, and A. L. Chernyshev, Disorder-induced Mimicry of a Spin Liquid in YbMgGaO₄, *Phys. Rev. Lett.* **119**, 157201 (2017).
- [19] E. Parker and L. Balents, Finite-temperature behavior of a classical spin-orbit-coupled model for YbMgGaO₄ with and without bond disorder, *Phys. Rev. B* **97**, 184413 (2018).
- [20] I. Kimchi, A. Nahum, and T. Senthil, Valence Bonds in Random Quantum Magnets: Theory and Application to YbMgGaO₄, *Phys. Rev. X* **8**, 031028 (2018).
- [21] I. Kimchi, J. P. Shekelton, T. M. McQueen, and P. A. Lee, Scaling and data collapse from local moments in frustrated disordered quantum spin systems, *Nat. Commun.* **9**, 4367 (2018).
- [22] Y. Li, G. Chen, W. Tong, L. Pi, J. Liu, Z. Yang, X. Wang, and Q. Zhang, Rare-Earth Triangular Lattice Spin Liquid: A Single-Crystal Study of YbMgGaO₄, *Phys. Rev. Lett.* **115**, 167203 (2015).
- [23] M. B. Sanders, F. A. Cevallos, and R. J. Cava, Magnetism in the KBaRE(BO₃)₂ (RE = Sm, Eu, Gd, Tb, Dy, Ho, Er, Tm, Yb, Lu) series: materials with a triangular rare earth lattice, *Mater. Res. Express* **4**, 036102 (2017).
- [24] S. Guo, T. Kong, and R. J. Cava, NaBaR(BO₃)₂ (R = Dy, Ho, Er and Tm): structurally perfect triangular lattice materials with two rare earth layers, *Mater. Res. Express* **6**, 106110 (2019).
- [25] S. Guo, T. Kong, F. A. Cevallos, K. Stolze, and R. J. Cava, Crystal growth, crystal structure and anisotropic magnetic properties of KBaR(BO₃)₂ (R = Y, Gd, Tb, Dy, Ho, Tm, Yb and Lu) triangular lattice materials, *J. Magn. Magn. Mater.* **472**, 104 (2019).
- [26] S. Guo, T. Kong, W. W. Xie, L. Nguyen, K. Stolze, F. A. Cevallos, and R. J. Cava, Triangular rare-earth lattice materials RbBaR(BO₃)₂ (R = Y, Gd, Yb) and comparison to the KBaR(BO₃)₂ analogs, *Inorg. Chem.* **58**, 3308 (2019).
- [27] S. Guo, A. Ghasemi, C. L. Broholm, and R. J. Cava, Magnetism on ideal triangular lattices in NaBaYb(BO₃)₂, *Phys. Rev. Mater.* **3**, 094404 (2019).
- [28] M. R. Norman, *Colloquium: Herbertsmithite and the search for the quantum spin liquid*, *Rev. Mod. Phys.* **88**, 041002 (2016).
- [29] Y. Ran, M. Hermele, P. A. Lee, and X. G. Wen, Projected-Wave-Function Study of the Spin-1/2 Heisenberg Model on the Kagome Lattice, *Phys. Rev. Lett.* **98**, 117205 (2007).
- [30] M. Sutherland, D. G. Hawthorn, R. W. Hill, F. Ronning, S. Wakimoto, H. Zhang, C. Proust, E. Boaknin, C. Lupien, L. Taillefer, R. X. Liang, D. A. Bonn, W. N. Hardy, R. Gagnon, N. E. Hussey, T. Kimura, M. Nohara, and H. Takagi, Thermal conductivity across the phase diagram of cuprates: Low-energy quasiparticles and doping dependence of superconducting gap, *Phys. Rev. B* **67**, 174520 (2003).
- [31] S. Y. Li, J. B. Bonnemaïson, A. Payeur, P. Fournier, C. H. Wang, X. H. Chen, and L. Taillefer, Low-temperature phonon thermal conductivity of single crystalline Nd₂CuO₄: Effects of sample size and surface roughness, *Phys. Rev. B* **77**, 134501 (2008).
- [32] K. M. Ranjith, S. Luther, T. Reimann, B. Schmidt, Ph. Schlender, J. Sichelschmidt, H. Yasuoka, A. M. Strydom, Y. Skourski, J. Wosnitza, H. Kühne, Th. Doert, and M. Baenitz, Anisotropic field-induced ordering in the triangular-lattice quantum spin liquid NaYbSe₂, *Phys. Rev. B* **100**, 224417 (2019).
- [33] P.-L. Dai, G. Zhang, Y. Xie, C. Duan, Y. Gao, Z. Zhu, E. Feng, C.-L. Huang, H. Cao, A. Podlesnyak, G. Granroth, D. Voneshen, S. Wang, G. Tan, E. Morosan, X. Wang, L. Shu, G. Chen, Y. Guo, X. Lu, and P. Dai, Spinon fermi surface spin liquid in a triangular lattice antiferromagnet NaYbSe₂, [arXiv:2004.06867](https://arxiv.org/abs/2004.06867).